

Checkpoint-dependent phosphorylation of Exo1 modulates the DNA damage response

This is an open-access article distributed under the terms of the Creative Commons Attribution License, which permits distribution, and reproduction in any medium, provided the original author and source are credited. This license does not permit commercial exploitation without specific permission.

Isabelle Morin^{1,6}, Hien-Ping Ngo^{1,6},
Amanda Greenall^{1,2}, Mikhajlo K Zubko^{1,3},
Nick Morrice⁴ and David Lydall^{1,2,5,*}

¹Institute for Ageing and Health, Henry Wellcome Laboratory for Biogerontology Research, Newcastle University, Newcastle Upon Tyne, UK, ²Centre for Integrated Systems Biology of Ageing and Nutrition, Henry Wellcome Laboratory for Biogerontology Research, Newcastle University, Newcastle Upon Tyne, UK, ³Division of Biology, School of Biology, Chemistry & Health Science, Faculty of Science and Engineering, Manchester Metropolitan University, Manchester, UK, ⁴MRC Protein Phosphorylation Unit, College of Life Sciences, University of Dundee, Dundee, UK and ⁵Institute for Cell and Molecular Biosciences, Henry Wellcome Laboratory for Biogerontology Research, Newcastle University, Newcastle Upon Tyne, UK

Exo1 is a nuclease involved in mismatch repair, DSB repair, stalled replication fork processing and in the DNA damage response triggered by dysfunctional telomeres. In budding yeast and mice, Exo1 creates single-stranded DNA (ssDNA) at uncapped telomeres. This ssDNA accumulation activates the checkpoint response resulting in cell cycle arrest. Here, we demonstrate that Exo1 is phosphorylated when telomeres are uncapped in *cdc13-1* and *yku70Δ* yeast cells, and in response to the induction of DNA damage. After telomere uncapping, Exo1 phosphorylation depends on components of the checkpoint machinery such as Rad24, Rad17, Rad9, Rad53 and Mec1, but is largely independent of Chk1, Tel1 and Dun1. Serines S372, S567, S587 and S692 of Exo1 were identified as targets for phosphorylation. Furthermore, mutation of these Exo1 residues altered the DNA damage response to uncapped telomeres and camptothecin treatment, in a manner that suggests Exo1 phosphorylation inhibits its activity. We propose that Rad53-dependent Exo1 phosphorylation is involved in a negative feedback loop to limit ssDNA accumulation and DNA damage checkpoint activation.

The EMBO Journal (2008) 27, 2400–2410. doi:10.1038/emboj.2008.171; Published online 28 August 2008

Subject Categories: genome stability & dynamics

Keywords: *cdc13-1*; checkpoint; Exo1; phosphorylation; telomere

Introduction

The DNA damage response is an evolutionarily conserved mechanism dedicated to cellular defence against genomic insults (Elledge, 1996; Nyberg *et al*, 2002; Rouse and Jackson, 2002). In yeast and mammals, different types of damage, for example double-stranded breaks (DSBs) or replication stalling, induce a DNA damage response that triggers cell cycle arrest and expression of genes required for DNA repair (Kolodner *et al*, 2002).

Primary DNA lesions are often processed by nucleases that generate single-stranded DNA (ssDNA). Thus, ssDNA is a common intermediate in DSB repair, nucleotide excision repair, recombination repair and at collapsed replication forks and is believed to have a key function in the DNA damage response (Lydall and Weinert, 1995; Lee *et al*, 1998; Pang *et al*, 2003). For example, upon DSB formation, the MRX complex (the Mre11–Rad50–Xrs2 complex in yeast, or the Mre11–Rad50–Nbs1 complex in humans) is thought to collaborate with the exonuclease Exo1 in the generation of 3'-ended ssDNA tracts at DSB ends, as a first step to initiate the repair process through homologous recombination (Ivanov *et al*, 1994; Lee *et al*, 1998; Tsubouchi and Ogawa, 2000; Lewis *et al*, 2002; Llorente and Symington, 2004; Schaezlein *et al*, 2007). ssDNA is coated with replication protein A (RPA) (Wang and Haber, 2004). RPA-covered DNA recruits the phosphatidylinositol 3-kinase-like protein kinase (PIKK) Mec1 (ATR in human cells) to a region near the DSB end (Zou and Elledge, 2003; Dubrana *et al*, 2007). A second set of proteins is required with Mec1 to initiate the DNA damage checkpoint and consists of a clamp (the Rad17–Mec3–Ddc1 complex) and a clamp loader (Rad24–RFC) (Majka *et al*, 2006). Mec1, in collaboration with the clamp and the clamp loader, activates the downstream kinases Rad53 and Chk1 with the assistance of the checkpoint mediator Rad9 (Sanchez *et al*, 1996; Sun *et al*, 1996; Sweeney *et al*, 2005). Activated Rad53 becomes hyperphosphorylated and is critical for halting cell cycle progression and for DNA repair in part through phosphorylation of downstream target kinase Dun1 (Lee *et al*, 2003; Chen *et al*, 2007).

Chromosome ends have to be distinguished from DSBs that are potent activators of DNA damage checkpoint. For this purpose, the telomere exerts an effect as a protective cap at the ends of linear eukaryotic chromosomes. Telomeres ensure genomic stability by protecting against end degradation, recombination and fusion (Blackburn, 2001; de Lange, 2005). In budding yeast, telomeric DNA is primarily made of a double-stranded DNA region of tandem TG_{1–3} repeats, known as the G strand, which extends beyond the duplex region, creating a short single-stranded 3' overhang (Blackburn *et al*, 1989). This 3' overhang is bound by a specific ssDNA-binding protein, Cdc13 (homologue of

*Corresponding author. Institute for Ageing and Health, Henry Wellcome Laboratory for Biogerontology Research, Newcastle University, Newcastle Upon Tyne NE4 6BE, UK. Tel.: +44 191 256 3449; Fax: +44 191 256 3445; E-mail: D.A.Lydall@ncl.ac.uk
⁶Joint first authors

Received: 3 December 2007; accepted: 30 July 2008; published online: 28 August 2008

mammalian Pot1), which protects telomeric ends and is also involved in recruiting telomerase complex (Nugent *et al*, 1996; Hockemeyer *et al*, 2005).

Dysfunctional telomeres (i.e. shortened or uncapped) are at the interface between ageing and cancer (Djojusbrotto *et al*, 2003). Dysfunctional telomeres trigger a DNA damage response resulting in senescence or apoptosis in mammalian cells and are thought to exert an effect in this way as a tumour suppressor mechanism (Campisi *et al*, 2001; Cosme-Blanco *et al*, 2007). In budding yeast, shortened telomeres also activate a DNA damage response, similar to the one triggered by DSBs (Ijima and Greider, 2003; Enomoto *et al*, 2004). Telomere uncapping induced in *Cdc13-1* defective cells (*cdc13-1* mutants) leads to long tracts of single-stranded 3' DNA at and near telomere ends (Garvik *et al*, 1995). The nuclease, Exo1, is involved in the generation of ssDNA and contributes to the activation of the DNA damage checkpoint in *cdc13-1* mutants (Maringele and Lydall, 2002; Zubko *et al*, 2004). In addition, Exo1 has functions at other kinds of budding yeast telomere capping defects (Maringele and Lydall, 2002, 2004; Bertuch and Lundblad, 2004; Tsolou and Lydall, 2007; Vega *et al*, 2007).

The parallel between budding yeast and mammalian cell responses to uncapped telomeres is strong, and was recently strengthened when a role for Exo1 at uncapped telomeres in mice was demonstrated. Exo1 was shown to participate in the formation of ssDNA, RPA recruitment and ATR activation in response to telomere dysfunction in mice (Schaetzlein *et al*, 2007). Furthermore, in this mouse model system, mice lacking Exo1 lived significantly longer than control mice expressing Exo1. This strongly suggests that regulation of Exo1 activity has the potential to affect mammalian cell responses to uncapped telomeres and mammalian lifespan.

How Exo1 activity is regulated is largely unknown. Two recent papers reported that human Exo1 was phosphorylated by ATR and degraded after treatment of cells by the S-phase inhibitor hydroxyurea (El-Shemerly *et al*, 2005, 2008). In addition, our previous work in budding yeast suggested the importance of part of the checkpoint kinase cascade, namely Mec1, Rad9 and Rad53, in inhibiting Exo1 at uncapped telomeres (Figure 1) (Jia *et al*, 2004; Zubko *et al*, 2004).

Here, we examine Exo1 post-translational modification triggered by telomere uncapping and DNA damage in budding yeast. We show that Exo1 is phosphorylated in a checkpoint-dependent manner when telomeres are unprotected. Phosphorylation is dependent on components of the clamp (Rad17), the clamp loader (Rad24), the mediator Rad9 and the downstream kinase Rad53 and is largely dependent on Mec1. We also show that Exo1 is phosphorylated by induction of DNA damage. Mutation of the residues in Exo1 that are phosphorylated suggests that Exo1 is inhibited by phosphorylation *in vivo* and that this phosphorylation has an important function in modulating the cellular response to DNA damage and uncapped telomeres.

Results

Exo1 is phosphorylated when telomeres are uncapped

Post-translational modifications (acetylation, phosphorylation, ubiquitination, glycosylation and so on) have a crucial function in a myriad of cellular processes by affecting the conformation, activity or stability of modified proteins (Mann

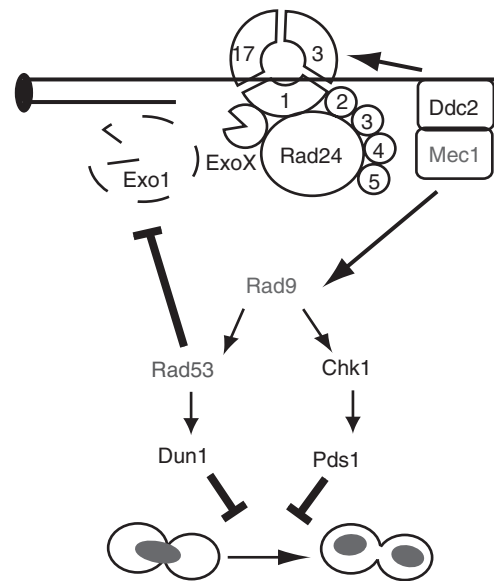


Figure 1 Inhibition of ssDNA formation at uncapped telomeres. A model based on that in Jia *et al* (2004) showing the function of DNA damage checkpoint proteins in signalling cell cycle arrest and inhibiting nuclease activities in response to *cdc13-1*-induced telomere uncapping. (17,3,1) represents the Rad17, Mec3 and Ddc1 hetero-trimeric PCNA-type ring. (2,3,4,5) represents the four small RFC subunits of the Rad24 complex. ExoX is an unidentified exonuclease, regulated by the checkpoint sliding clamp. Other proteins are as indicated.

and Jensen, 2003). In particular, the DNA damage response involves a protein phosphorylation cascade propagated through protein kinases, most importantly Mec1, Rad53 and Chk1 in budding yeast (Longhese *et al*, 1998).

To determine whether the nuclease Exo1 is modified when telomeres are uncapped, we examined the electrophoretic mobility of Exo1 by western blot. For this purpose, a C-terminal Myc epitope was inserted at the *EXO1* chromosomal locus in a *cdc13-1* strain and the functionality of this modified allele was addressed by spot tests (Figure 2A). At the restrictive temperatures of 26 and 27°C, the growth of *cdc13-1 EXO1-myc::HIS3* strains was most similar to that of *cdc13-1 EXO1* strains but clearly much less than *cdc13-1 exo1Δ* strains. This demonstrates that Exo1-Myc is functional in the context of telomere capping defects.

Telomere uncapping was induced in a *cdc13-1 EXO1-myc::HIS3* strain by growth at 36°C and the mobility of Exo1 was measured by western blot. At different times, samples were collected and subjected to immunoblotting. As shown in Figure 2B, optimized conditions allowed us to detect a subtle but reproducible slower migrating form of Exo1 after 2, 4 and 6 h at 36°C. Rad53, the budding yeast Chk2 kinase, which is phosphorylated and activated as part of the budding yeast DNA damage response, was phosphorylated in this assay with similar kinetics. As a control, we confirmed that this modified form of Exo1 was not due to heat shock as it was not observed after culture of a *CDC13* strain expressing Exo1-Myc at 36°C for 6 h (data not shown). We conclude that Exo1 is modified after telomere uncapping and this modification is associated with a mobility shift detectable by western blot.

To determine whether the modified form of Exo1 observed after telomere uncapping is due to phosphorylation, we next

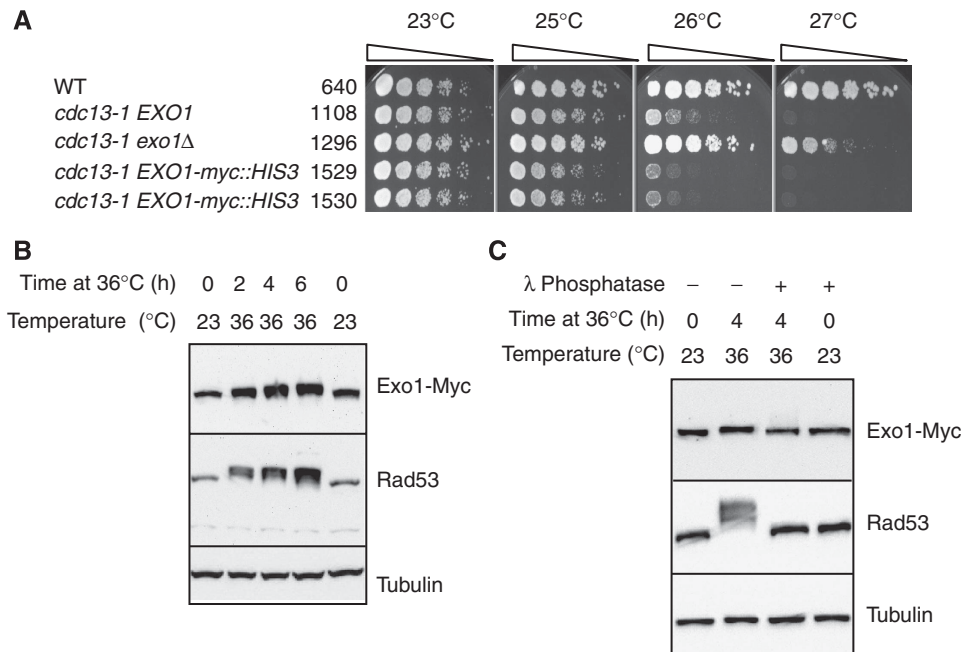


Figure 2 Exo1-Myc is phosphorylated when telomeres are uncapped. (A) Six-fold serial dilutions of the indicated strains were spotted onto YPD plates and grown for 2 days at the indicated temperatures before being photographed. (B) A *cdc13-1 EXO1-myc::HIS3* (DLY1529) strain, exponentially growing at 23°C, was grown for a further 6 h at 23°C or transferred at 36°C for 2, 4 or 6 h to induce telomere uncapping. Total protein lysates were prepared by TCA extraction, separated on 7.5% SDS-PAGE and blotted on nitrocellulose membrane. Exo1-Myc, Rad53 and tubulin were detected by western blot. (C) Native protein extracts from culture of a *cdc13-1 EXO1-myc::HIS3 pep4Δ* strain (DLY3259) grown at 23 or 36°C for 4 h were incubated with lambda phosphatase (+ λ phosphatase). Exo1-Myc, Rad53 and tubulin were detected by western blot.

evaluated the sensitivity of Exo1 shift to lambda phosphatase. For this experiment, we used a *cdc13-1* yeast strain deleted for the protease *PEP4* to avoid degradation of Exo1, observed *in vitro* when proteins were extracted in non-denaturing conditions after culture at 36°C for more than 3 h (data not shown). Native protein extracts from a *cdc13-1 pep4Δ EXO1-myc::HIS3* strain incubated at 23 or 36°C were treated with lambda phosphatase. We found that phosphatase treatment returned the modified form of Exo1 to its faster migrating original form, indicating that Exo1 is indeed phosphorylated (Figure 2C). The phosphatase treatment also reduced the mobility shift of Rad53. These findings indicate that Exo1 is phosphorylated when telomere uncapping is induced in a Cdc13-defective strain.

Exo1 phosphorylation is dependent on components of the checkpoint machinery

Cells respond to DNA damage and uncapped telomeres by the activation of checkpoint kinase cascades. Therefore, we decided to investigate the dependency of Exo1 phosphorylation on checkpoint genes. For this purpose, *cdc13-1* yeast strains expressing Exo1-Myc and deleted for *RAD24*, *RAD17*, *RAD9*, *RAD53*, *MEC1*, *TEL1*, *DUN1* or *CHK1* were created. The lack of viability of *mec1Δ* and *rad53Δ* cells was rescued by deleting the *SML1* gene, which causes an increase in dNTP synthetic capacity (Zhao *et al*, 1998). For each genetic background, Exo1 phosphorylation was assessed, in duplicate strains, by western blot. In parallel, we examined Rad53 phosphorylation in the same extracts. As shown in Figure 3A, *RAD9*, *RAD17*, *RAD24* and *RAD53* were all required for Exo1 phosphorylation upon telomere uncapping. Thus, Exo1 phosphorylation is dependent on components of the clamp loader (Rad24), the clamp (Rad17), the mediator Rad9 and the effector kinase

Rad53. In addition, deletion of *MEC1* largely reduces Exo1 phosphorylation, and *mec1Δ tel1Δ* double mutants show no phosphorylation (Figure 3B). Finally, Figure 3C shows that deletions of *TEL1*, *CHK1* or *DUN1* do not strongly affect Exo1 phosphorylation after telomere uncapping.

Interestingly, there is a strong correlation between Rad53 and Exo1 phosphorylation in all experiments (i.e. significant Exo1 phosphorylation is detected when Rad53 is phosphorylated at high levels and vice versa (Figures 3A and C)). This correlation suggests that the kinase responsible for Exo1 phosphorylation is either Rad53 or a kinase downstream of Rad53 (other than Dun1; Figure 3C). To test this hypothesis, we examined Exo1 phosphorylation in a cell that contained the *rad53K227A* (kinase dead) allele and *cdc13-1* mutant at restrictive temperature (Figure 3D). We observed that Exo1 was not phosphorylated in a strain containing the *rad53K227A* allele, suggesting that Rad53, or a kinase downstream of Rad53, is responsible for phosphorylating Exo1 after telomere uncapping. However, we were not able to detect a direct interaction with Exo1 and Rad53 or Rad53KD by immunoprecipitation (data not shown).

In summary, Exo1 is phosphorylated in response to telomere uncapping and this phosphorylation relies on the DNA damage checkpoint proteins Rad24, Rad17, Rad9, Rad53 and Mec1.

Exo1 phosphorylation is activated by a variety of genomic insults

To determine whether Exo1 phosphorylation was specific to deprotection of the 3' overhang in the *cdc13-1* system, other kinds of genomic stresses were induced in *CDC13* cells. First, telomeres were uncapped in a mutant deleted for *YKU70*. The conserved Ku70/Ku80 heterodimer is involved in telomere

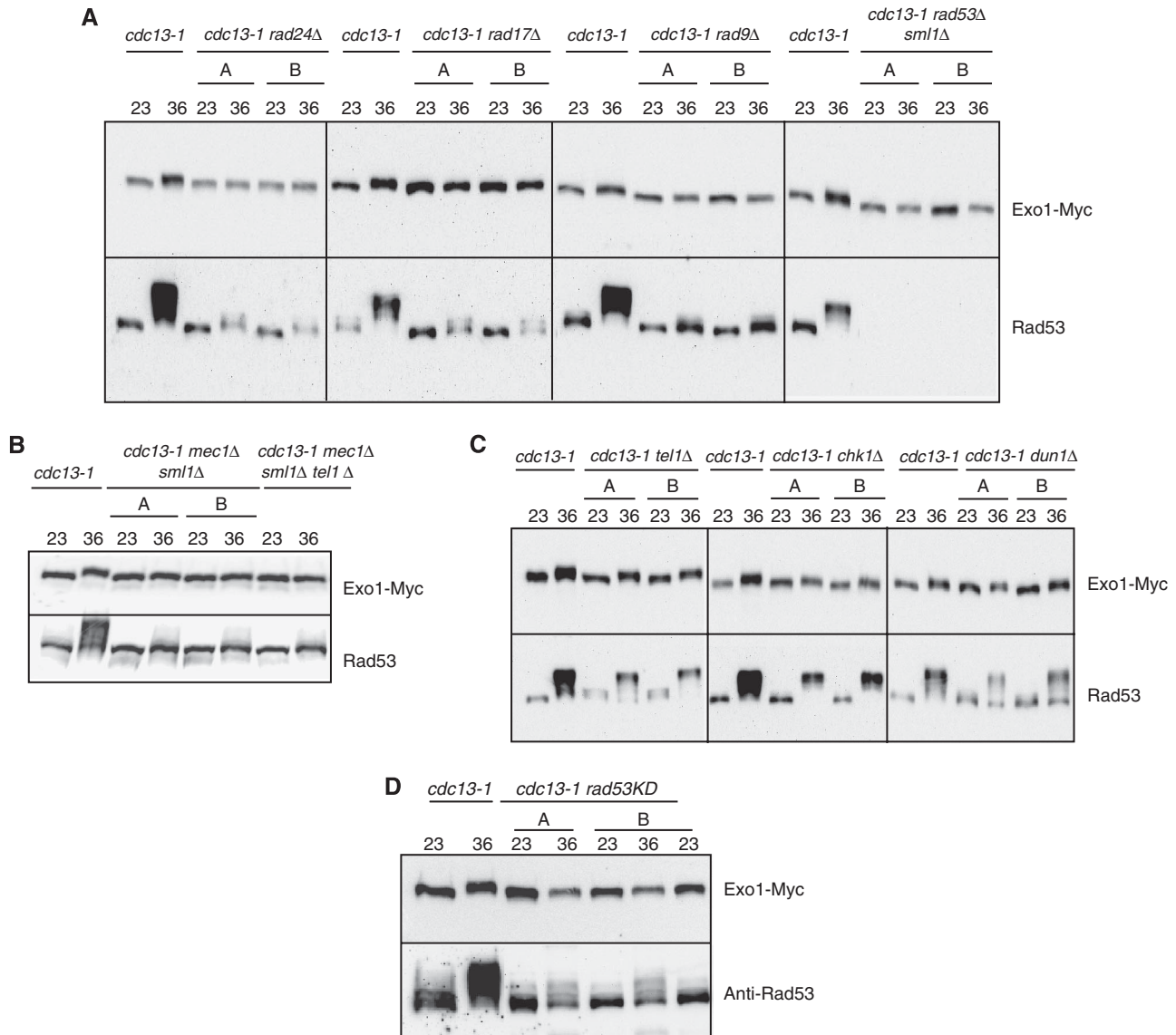


Figure 3 The phosphorylation of Exo1 is checkpoint dependent. All strains carried *EXO1-myc::HIS3*. For each experiment, two different strains with the same genotype, indicated as A and B were examined. (A) *cdc13-1* (DLY1529) and *cdc13-1 rad24Δ* (DLY2974 and DLY2975), *cdc13-1 rad17Δ* (DLY3844 and DLY3845), *cdc13-1 rad9Δ* (DLY3009 and DLY3010), *cdc13-1 rad53Δ sml1Δ* (DLY3073 and DLY3074), strains exponentially growing at 23°C, were grown for a further 6 h at 23 or 36°C. Western blots of TCA protein extracts were first probed with anti-Myc antibodies to detect Exo1-Myc. Membranes were stripped and reprobed with anti-Rad53 antibodies. (B) As in (A) but with *cdc13-1 mec1Δ sml1Δ* strains (DLY4146 and DLY3261) and *cdc13-1 mec1Δ sml1Δ tel1Δ* strains (DLY4115). (C) As in (A) but with *cdc13-1 tel1Δ* (DLY3002 and DLY3003), *cdc13-1 chk1Δ* (DLY3011 and DLY3012), *cdc13-1 dun1Δ* strains (DLY3077 and DLY3078). (D) As in (A) but with *cdc13-1 Rad53KD* strain (DLY3568 and DLY3569).

end protection, and involved in the non-homologous end joining DNA repair process (Boulton and Jackson, 1996; Jeggo, 1998; Hsu *et al*, 1999; Fisher and Zakian, 2005). At high temperatures, yeast strains defective in Ku uncapped their telomeres, induce Exo1-dependent ssDNA formation, and activate cell cycle arrest (Maringele and Lydall, 2002). Importantly, Exo1 phosphorylation is detected when *yku70Δ* mutant cells expressing Exo1-Myc are grown at 37°C for 6 h (Figure 4A). We conclude that Exo1 is phosphorylated in response to different types of telomere capping defects in budding yeast.

Exo1 is involved in mismatch repair (Fiorentini *et al*, 1997; Tran *et al*, 2004), DSB repair (Tsubouchi and Ogawa, 2000; Llorente and Symington, 2004) and at stalled replication forks (Cotta-Ramusino *et al*, 2005; Bermejo *et al*, 2007). Therefore,

we tested whether Exo1 was phosphorylated after genomic insults other than telomere uncapping. Figure 4B indicates that Exo1 phosphorylation is observed after treatment with the DSB-inducing agent bleomycin. To study defects in DNA replication, we examined yeast cells defective in DNA ligase Cdc9 (*cdc9-1*) (Johnston and Nasmyth, 1978). When grown at the restrictive temperature of 36°C, DNA replication is defective in *cdc9-1* mutants and Exo1 phosphorylation is detected (Figure 4B). Importantly, Exo1 phosphorylation was not detected when cells were treated with nocodazole or alpha factor, showing that cell cycle arrest in G2/M or G1 does not induce Exo1 phosphorylation (Supplementary Figure 1). Taken together, our data clearly show that Exo1 phosphorylation is a common response to DNA damage caused by a variety of genomic insults.

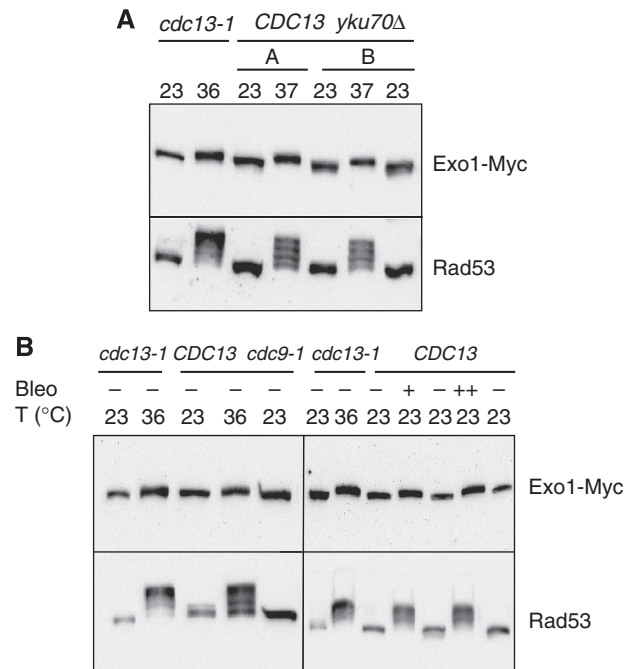


Figure 4 Exo1 phosphorylation is induced by a range of genomic insults. All strains carried *EXO1-myc::HIS3*. (A) A *cdc13-1* (DLY1529) and *CDC13 yku70Δ* strain (DLY3405 and DLY3406), exponentially growing at 23°C, were grown for a further 6 h at 23°C or transferred at higher temperature (36 and 37°C) to induce telomere uncapping. Western blots were performed as in Figure 3 and two different strains with the same genotype, indicated as A and B were examined. (B) *cdc13-1* (DLY1529), exponentially growing at 23°C, was transferred to 36°C for 6 h. Left panel: cell cultures of *CDC13 cdc9-1* (DLY3262), exponentially growing at 23°C, were transferred to 36°C for 6 h. Right panel: cell cultures of *CDC13* (DLY3079) were grown at 23°C in YPD and transferred into YPD with bleomycin (50 µg/ml), samples were taken at 2 h (+) and 4 h (+ +). Western blots of TCA protein extracts were first probed with anti-Myc antibodies to detect Exo1-Myc. Membranes were stripped and reprobed with anti-Rad53 antibodies.

Exo1 is phosphorylated on specific sites in response to uncapped telomeres

To understand why and how Exo1 is phosphorylated in response to telomere uncapping, it was important to determine the identity of the phosphorylated sites. For this purpose, Exo1 was purified using a TAP epitope fused in frame at the C terminus (Rigaut *et al*, 1999). A *cdc13-1 EXO1-tap::URA3* strain was created and the functionality of Exo1-Tap was assessed by spot tests. As shown in Figure 5A, *cdc13-1 EXO1-tap::URA3* and *cdc13-1 EXO1* strains grew similarly showing that Exo1-Tap is functional. To avoid degradation of Exo1 when incubating cells for more than 3 h at 36°C, we also used a strain deleted for *PEP4*, coding for the vacuolar protease Pep4 (Figure 5A). *cdc13-1 EXO1-tap::URA3* strains were grown at 23°C or at 36°C for 3 h and a 'quick' TAP purification was performed to preserve as many post-translational modifications as possible (Materials and methods). Figure 5B lane 1 shows TAP purification from cells grown at 23°C, lane 3 shows samples grown at 36°C and lane 5 is a control purification from a non-epitope-tagged strain. Lanes 1 and 3 show a single extra band, marked with a star, not detected in the control lane (lane 5). This band was identified as Exo1-Tap by western blot (data not shown). Purification of Exo1 did not reveal any other

extra band(s), suggesting that we were not able to identify any protein partners of Exo1 either in exponentially dividing cells or in cells arrested at the checkpoint due to telomere uncapping.

The Exo1-Tap bands from lanes 1 and 3 and from a *cdc13-1 EXO1-tap::URA3 pep4Δ* strain grown for 4 h at 36°C (not shown) were excised and digested with trypsin. The digests were analysed by LC-MS with precursor 79 scanning as described previously (Williamson *et al*, 2006). The tryptic digests were also analysed on an LTQ-orbitrap mass spectrometer coupled to a Dionex 3000 nano LC system (Materials and methods). As shown in Figure 5C, a dramatic increase is seen in the peak intensities for phosphorylated Exo1, purified when telomere uncapping was induced (grey line, compared with red line, 23°C control). We mapped four distinct major phosphorylation sites induced in Exo1 after telomere uncapping and the same residues in Exo1 were identified after culture of a *cdc13-1 EXO1-tap::URA3 pep4Δ* strain for 4 h at 36°C. We conclude four phosphorylated serines, S372, S567, S587 and S692, are major targets of the DNA damage response triggered by uncapped telomeres in a *Cdc13*-defective strain. Consistent with our results, others identified S372, but no other residues in Exo1, in a proteomic screen for budding yeast DNA damage checkpoint kinase targets after treatment of cells with the alkylating agent MMS (Smolka *et al*, 2007).

Exo1 phosphorylation mutant alleles exhibit different responses to telomere uncapping and DNA damage

To examine the effect of Exo1 phosphorylation on the DNA damage response, we mutated Exo1 phosphorylation sites. The *EXO1-tap* construct and 900 bp upstream was amplified from yeast by PCR and subcloned in the single-copy vector pRS413 to create pRS413-Exo1-Tap. We checked by western blot that Exo1 expression level by the pRS413-Exo1-Tap in *cdc13-1 exo1Δ* was similar to the expression level generated by the integrated *EXO1-tap* allele (Supplementary Figure 2). The four serine residues S372, S567, S587 and S692 were converted into alanine (Exo1-4S::A-Tap) or glutamic acid (Exo1-4S::E-Tap). Conversion of serine to alanine blocks the phosphorylation on these residues, whereas the negative charge of the glutamic acid mimics the negative charge carried by a phosphorylated serine residue.

The growth of *cdc13-1 exo1Δ* strains expressing WT Exo1-Tap, Exo1-4S::A-Tap or Exo1-4S::E-Tap on centromeric plasmids was analysed, in duplicate, by spot tests at a range of temperatures (Figure 6A). *cdc13-1 exo1Δ* strains expressing Exo1-Tap or mutants grew less well than *cdc13-1 exo1Δ* carrying the empty vector pRS413 at 28°C (data not shown). We conclude that Exo1-Tap, Exo1-4S::A-Tap and Exo1-4S::E-Tap are all functional. However, at 27°C and particularly noticeable at 26.5°C, we detected differences in growth between cells expressing Exo1-Tap, Exo1-4S::A-Tap or Exo1-4S::E-Tap. At 26.5°C, *cdc13-1* strains expressing Exo1-4S::A-Tap grow poorly compared with *cdc13-1* expressing Exo1-Tap and Exo1-4S::E-Tap. We can conclude from this, and our observation that overexpression of Exo1 is detrimental to the growth of the *cdc13-1* mutants (Supplementary Figures 3 and 4), that Exo1-4S::A is more active than either Exo1 or Exo1-4S::E. In addition, we also found that *cdc13-1* strain expressing Exo1-4S::E-Tap grew better than *cdc13-1* expressing Exo1-4S::A-Tap or Exo1-Tap at 26 and 26.5°C. The effects of Exo1 mutations are subtle but

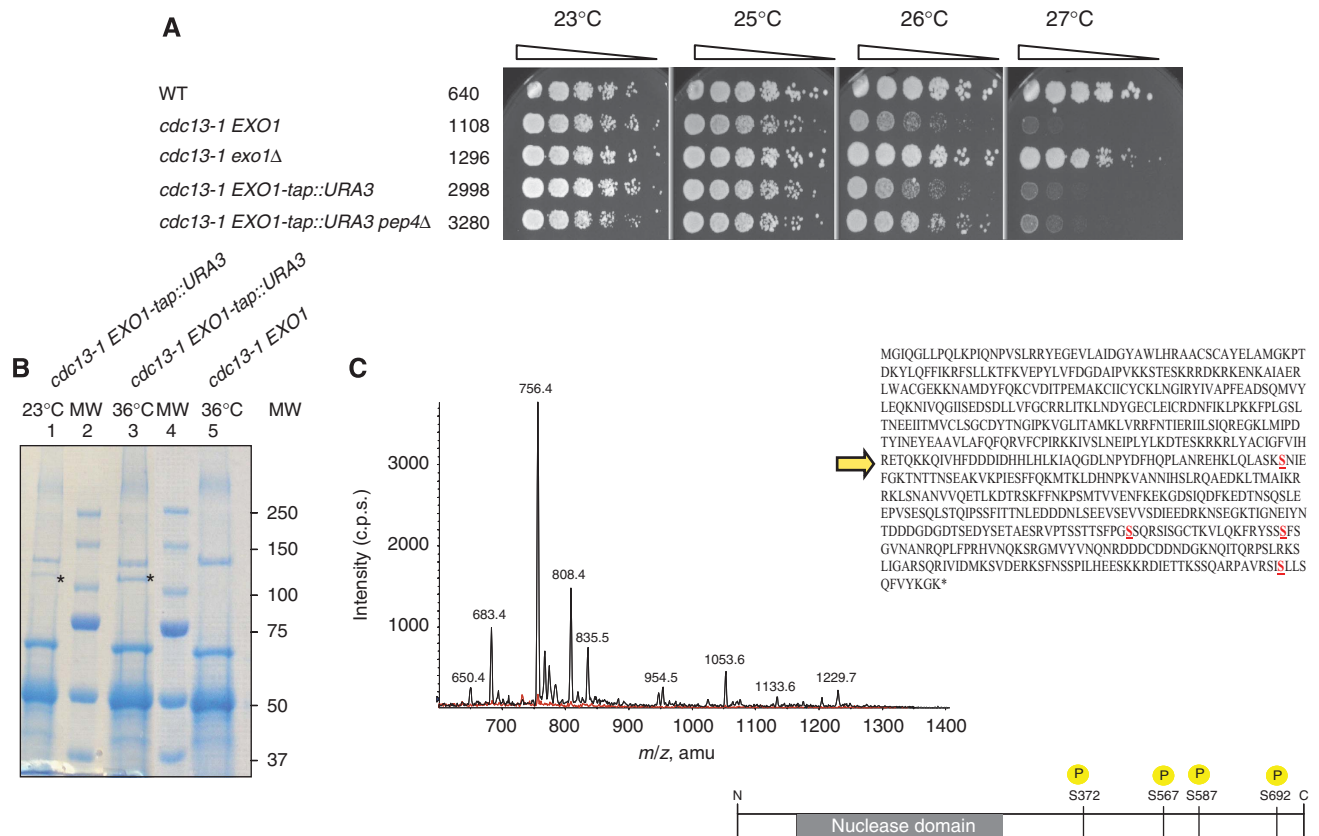


Figure 5 Identification of Exo1-phosphorylated sites upon telomere uncapping. **(A)** Spot test shows six-fold serial dilutions of the indicated strains on YPD grown for 3 days at the indicated temperatures. **(B)** *cdc13-1 EXO1-tap::URA3* strain (DLY2998) (31), growing exponentially at 23°C, was further incubated at 23°C or transferred to 36°C for 3 h. Low stringency purification of Exo1Tap was performed (lanes 1 and 3). A band identified as Exo1-Tap from lanes 1 and 3 is indicated by a star. Lanes 2 and 4 show molecular weight (MW) markers and sizes are indicated on the right. Lane 5 is a control and shows proteins extracted from a culture of *cdc13-1 EXO1* strain (DLY1108) grown for 3 h at 36°C. **(C)** Exo1 bands, similar to those shown in **(B)**, at 23°C (lane 1, *) and at 36°C (lane 3, *) were analysed by mass spectrometry. The extracted ion chromatograms for the phosphopeptide ions detected by precursor ion scanning are shown for the tryptic digests of Exo1 grown at 23°C (red trace) or cultured for 3 h at 36°C (grey trace). The masses of the detected peptides are average masses (*m/z*) for the doubly negatively charged peptide ions ([M-2H]²⁻). Identity of phosphorylated serine residues are shown as red and underlined in Exo1 sequence.

reproducible and are consistent with the idea that Exo1 phosphorylation reduces the ability of Exo1 to respond to uncapped telomeres.

To better test the effects of serine to alanine or serine to glutamic acid mutations in Exo1, we integrated the alleles into the normal *EXO1* chromosomal locus. First, we showed that strains carrying a truncated Exo1 (*exo1Δ 1091–2109*), which was used to generate the mutated *EXO1* strains, showed a loss of function similar to *exo1Δ* strains (Figure 6B). We found that Exo1-4S::E was less functional than Exo1 when expressed from the normal locus because *cdc13-1 exo1-4S::E* mutants formed larger colonies than *cdc13-1 EXO1* strains at 26 and 26.5°C. However, we were unable to observe an effect of the *exo1-4S::A* mutations, at the *EXO1* locus, in *cdc13-1* mutants.

To test whether the phosphorylation of Exo1 affected responses to other types of DNA damage, we treated cells with the topoisomerase I poison camptothecin. This drug is believed to exert its toxicity through the generation of replication-associated DSBs (Pommier *et al*, 2003). Under this condition, DNA end resection by Exo1 and the ensuing repair is expected to be beneficial to cell growth and survival. This view is supported by the findings that strains carrying *EXO1* truncation or deletion show sensitivity to camptothecin

(Figure 6C and data not shown). After camptothecin treatment, we found that cells expressing Exo1-4S::A from the chromosomal locus were slightly more resistant to treatment compared with *EXO1* strains, whereas the strains expressing Exo1-4S::E were more sensitive than *EXO1* strains (Figure 6C). Although subtle, these results obtained from plasmid and integrated alleles strongly suggest that Exo1 phosphorylation inhibits the activity of Exo1 in response to telomere uncapping and camptothecin treatment.

One explanation for the comparatively subtle effects of the Exo1-4S::A and Exo1-4S::E mutations might be that other serine (threonine or tyrosine) residues were phosphorylated when the primary kinase targets had been mutated. Consistent with this idea, there are 61 serines, 36 threonines and 21 tyrosines in Exo1. To test this hypothesis, we epitope-tagged *exo1-4S::A* and *exo1-4S::E* alleles at the *EXO1* locus with the Myc epitope. In response to telomere uncapping, there was a clear increase in mobility of both Exo1-4S::A-Myc and Exo1-4S::E-Myc (Figure 6D). We conclude that in the absence of the primary phosphorylation targets Exo1 is modified at additional positions. Taken together, all our data suggest that Exo1 phosphorylation is regulated by and regulates the DNA damage response upon telomere uncapping and after treatment with camptothecin.

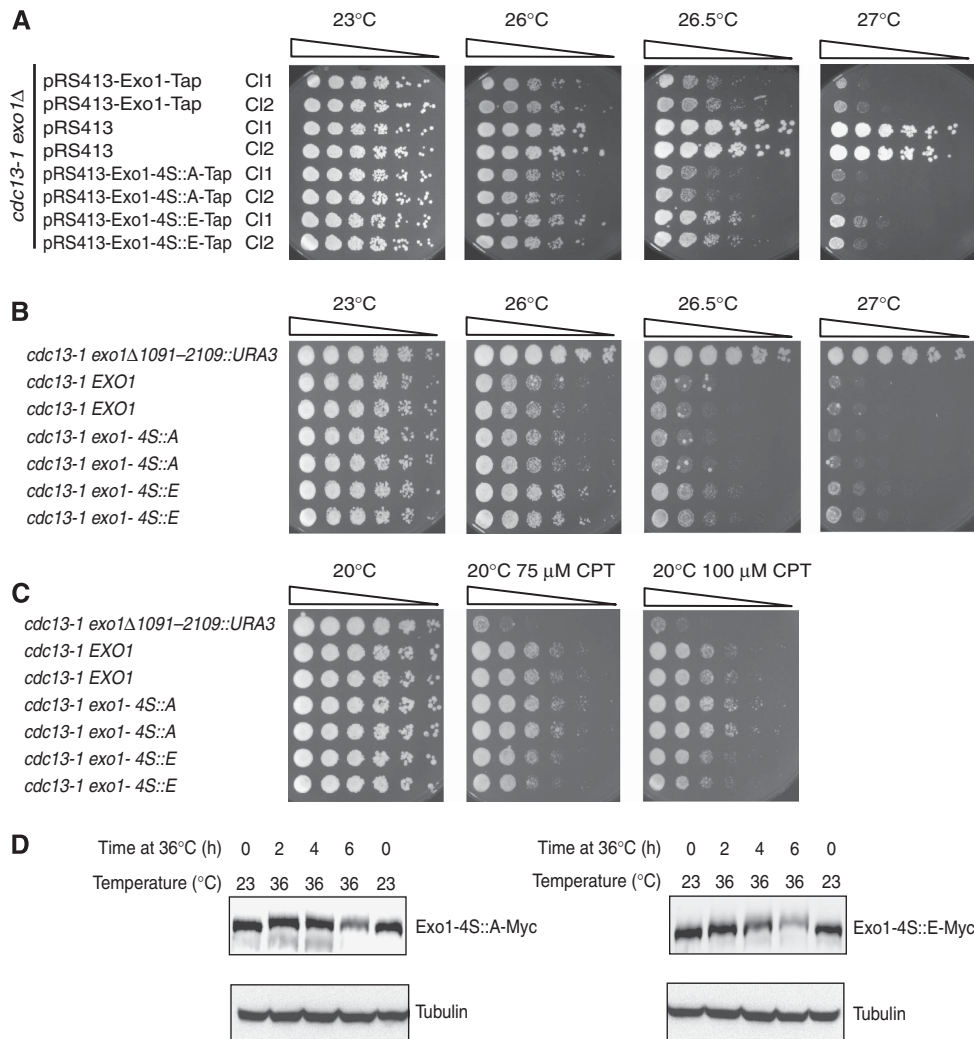


Figure 6 Exo1 phosphorylation mutant alleles exhibit different responses to telomere uncapping and DNA damage. **(A)** Spot test shows six-fold serial dilutions of *cdc13-1 exo1Δ* (DLY1296) strains carrying pRS413-Exo1-Tap, pRS413, pRS413-Exo1-4S::A-Tap or pRS413-Exo1-4S::E-Tap. Two independent transformant clones are shown (Cl1 and Cl2) and are representative of 10 clones tested in each case. **(B)** Spot test shows six-fold serial dilutions of *cdc13-1 exo1Δ1091-2109::URA3* (DLY4008), *cdc13-1 EXO1* (DLY4067), *cdc13-1 exo1-4S::A* (DLY4068) and *cdc13-1 exo1-4S::E* strains (DLY4069 and DLY4070). The plates were incubated at the temperature indicated for 2 days before the photographs were taken. **(C)** Spot test shows six-fold serial dilutions of *cdc13-1 exo1Δ1091-2109::URA3* (DLY4008), *cdc13-1 EXO1* (DLY4067), *cdc13-1 exo1-4S::A* (DLY4068) and *cdc13-1 exo1-4S::E* strains (DLY4069 and DLY4070). The plates were incubated for 4 days at 20°C before the photographs were taken. **(D)** *cdc13-1 exo1-4S::A-myc::HIS3* (DLY4138) and *cdc13-1 exo1-4S::E-myc::HIS3* (DLY4096) strains, exponentially growing at 23°C, were grown for a further 6 h at 23°C or transferred to 36°C for 2, 4 or 6 h. Total protein lysates were prepared by TCA extraction, separated on 7.5% PAGE and blotted onto nitrocellulose membrane. Exo1-Myc and tubulin were detected by western blot as in Figures 2–4.

Discussion

The DNA damage response is a powerful intracellular network that has the potential to repair damage, induce cell cycle arrest and in some cell types, induce apoptosis or senescence. To ensure that the DNA damage response works to the benefit of its host cell and organism, it is essential that responses to DNA damage are appropriately measured and properly regulated. Here, we show that Exo1, an evolutionarily conserved double strand-specific 5' to 3' exonuclease, involved in mismatch repair, DSB repair, meiosis and in responding to stalled replication forks and uncapped telomeres, is targeted and phosphorylated by the DNA damage checkpoint pathway.

Previous experiments have shown that Exo1 is critical for generating ssDNA at three classes of uncapped telomeres in budding yeast (*cdc13-1*, *yku70Δ* and telomerase knockout, *tlc1Δ*, cells; Maringele and Lydall, 2002, 2004; Bertuch and

Lundblad, 2004; Zubko *et al*, 2004). Exo1-dependent ssDNA appears to be a stimulus for the DNA damage checkpoint that results in cell cycle arrest in all three cases. In a similar way in mice, Exo1-dependent ssDNA formation amplifies the DNA damage signal at dysfunctional telomeres (Schaezlein *et al*, 2007).

Here, we show that a subset of DNA damage checkpoint proteins, Mec1, Rad17, Rad24, Rad9 and Rad53, has a crucial function in Exo1 phosphorylation and consequently modulates the accumulation of ssDNA at uncapped telomeres (this paper and Jia *et al*, 2004). Other checkpoint proteins, Dun1, Chk1 and Tel1 do not have an important function in this process.

We found that Exo1 was strongly phosphorylated on residues S372, S567, S587 and S692 in the C terminus. The phenotype of mutating these residues to alanines, to prevent phosphorylation, or glutamic acids, to mimic phosphorylation,

was subtle but indicated that Exo1 phosphorylation inhibits Exo1 *in vivo*. We propose that Exo1 phosphorylation limits the accumulation of ssDNA at unprotected telomeres, and therefore participates in a negative feedback loop to limit DNA damage checkpoint activation. Consistent with this conclusion, we find that expression of Exo1-4S::A and overexpression of Exo1 hyperactivates the DNA damage response in cells with uncapped telomeres (Supplementary Figures 3–5).

As Exo1 is a protein involved in many different DNA repair pathways, we suggest that Exo1 modification may exert an effect to downregulate Exo1 activity after many different kinds of damage. Such a modification would also exert an effect to limit the accumulation of ssDNA at damaged DNA. Consistent with this hypothesis, we observed Exo1 phosphorylation after treatment with the DSB-inducing agent, bleomycin and after inactivation of DNA ligase I. We also show that altering Exo1 phosphorylation affects sensitivity to camptothecin, in a manner that again suggests inhibitory role of phosphorylation on Exo1 activity (Figure 6C).

There are several possible mechanisms by which charge effects caused by phosphorylation of Exo1 might inhibit its activity. The most direct would be if phosphorylation of Exo1 inhibited the 5' to 3' exonuclease activity exhibited by Exo1. Phosphorylation of the C terminus might induce conformational changes that affect the recruitment of Exo1 to DNA and/or inhibit Exo1 activity. Another mechanism would be if the phosphorylation of Exo1 affects the ability of Exo1 to move through chromatin. As DNA damage induces chromatin modifications near DNA lesions, it seems conceivable, and indeed perhaps desirable, that chromatin structure near DNA damage prevents access of phosphorylated Exo1. Such an interaction would exert an effect to limit the accumulation of ssDNA near uncapped telomeres, DSBs or other types of lesions. Another possibility is that phosphorylation of Exo1 affects interaction of Exo1 with other proteins, for example, a nuclease activator or inhibitor. It has been reported previously that interactions between Exo1 and the mismatch repair proteins Mlh1 and Msh2 involve the Exo1 C terminus (Tishkoff *et al*, 1997; Schmutte *et al*, 2001; Tran *et al*, 2001, 2002). As the four phosphorylated serine residues have been identified at Exo1 C terminus, we can envisage that phosphorylation may affect the interactions between Exo1 and Mlh1 or Msh2. Finally, two recent studies in mammalian cells reported that Exo1 is ubiquitinated, and degraded, after DNA is damaged in the presence of hydroxyurea (El-Shemerly *et al*, 2005, 2008). In many cases, phosphorylation is an important signal for proteins to be recognized as targets by the proteasome–ubiquitin pathway. It seemed plausible that ubiquitination and degradation may indeed occur for budding yeast Exo1 and contribute to its inhibition. However, we saw no degradation of Exo1 when proteins were extracted in denaturing conditions (TCA) after telomere uncapping. The degradation we observed *in vitro* when proteins were extracted in native conditions after 4 h at 36°C was dependent on the vacuolar protease *PEP4*.

In conclusion, regulation of Exo1 upon telomere uncapping involves checkpoint-dependent phosphorylation, leading to the inhibition of Exo1. We believe that Rad53 (homologue of Chk2 in human cells) has a key function in this process and is most likely the kinase responsible for Exo1 phosphorylation. Examples are beginning to be identified where targets of the DNA damage response regulate DNA

damage processing. For example, the mammalian homologous recombination protein, BRCA1, is phosphorylated by Chk2 and this seems to affect whether homologous recombination or non-homologous end joining pathways are used to repair DSBs (Wang *et al*, 2006; Zhuang *et al*, 2006). If our experiments in yeast can be extrapolated to mammalian cells, we suggest that Chk2 inhibitors may affect the generation of ssDNA as well as downstream aspects of cell cycle arrest pathways in cells with telomere capping defects. Therefore, Chk2 inhibitors may also, similar to Exo1 deletion does in mice and yeast cells, improve the vitality of cells and animals with telomere capping defects, and perhaps, have a positive effect on mammalian ageing.

Materials and methods

Yeast strains

All the strains used in this study are in the W303 genetic background and are *RAD5+*, unless otherwise stated in Supplementary Table 1. A Myc epitope containing 13 copies was amplified by PCR using the plasmid pFA6a-13Myc-His3MX6 as a template (Longtine *et al*, 1998). The PCR product carrying the *HIS3* marker was transformed into *cdc13-1* yeast strain to generate *cdc13-1 EXO1-myc::HIS3* strains expressing Exo1-Myc (DLY1529 and DLY1530). Similarly, a Tap epitope was amplified by PCR using the plasmid pBS1539 as a template (Puig *et al*, 2001). The PCR product carrying the *URA3* marker was then transformed into *cdc13-1* strain to generate the strain *cdc13-1 EXO1-tap::URA3* (DLY2998). Correct integration was checked by PCR and/or Southern blot. Standard genetic crosses were used to obtain all the other strains from this study.

Cell cultures

Asynchronous cells were grown in YPD or selective medium until they reached the exponential growth rate ($OD_{600} = 0.8$). Then different treatments were applied. To induce telomere uncapping, *cdc13-1* and *yku70Δ* strains are incubated at the temperatures indicated in the figures. For cells treated with damaging agents, bleomycin (50 µg/ml; Sigma; 203408) was added to the cells for 2 or 6 h.

Cell lysis under denaturing conditions and western blot analysis

Protein extracts were prepared by glass bead breakage in TCA, essentially as previously described (Foiani *et al*, 1994). Briefly, cells were collected, washed once in water and resuspended in 10% TCA. Cells were mechanically broken using glass beads. Protein suspensions were pelleted, resuspended in Laemmli buffer (Bio-Rad; 161-0737) and the pH was equilibrated using Tris 1 M. Samples were boiled for 3 min, centrifuged for 10 min at 3000 r.p.m. and the supernatant was retained as the protein extract. For western blotting, proteins were separated on 7.5% SDS–PAGE (Bio-Rad; 161-1172). Gels were run for 2.5 h at 30 mA to maximize as much as possible the mobility shift between phosphorylated Exo1 and the non-phosphorylated form of Exo1. C-Myc antibody 9E10 was from Cancer Research UK. Peroxidase–anti-peroxidase soluble complex antibody from Sigma (P1291) was used to detect the TAP epitope. Antibodies against Rad53 were from Dan Durocher, Toronto. Anti-tubulin antibodies from Keith Gull, Oxford.

Cell lysis in non-denaturing conditions and dephosphorylation assay

Native protein extraction resulted in low yields of Exo1 in *cdc13-1* mutants grown at 36°C for more than 3 h. To improve yields, we deleted *PEP4*, encoding a vacuolar protease in *cdc13-1 EXO1-myc::HIS3 pep4Δ* strain (DLY3280). Yeast strain *cdc13-1 EXO1-myc::HIS3 pep4Δ* was then grown for 4 h at 23 or 36°C and whole-cell extracts were prepared by glass bead beating in a non-denaturing lysis buffer LB (Hepes 20 mM, NaCl 0.15 M, glycerol 10%, Tween 0.1%, phenylmethylsulphonyl fluoride 1 mM, protease inhibitor mixture (Roche Applied Science)). The dephosphorylation assays were carried out by incubating 50 µg of protein extracts in lambda phosphatase buffer supplemented with 2 mM $MnCl_2$ containing 1 µl of lambda phosphatase (λ -PPase; New England

Biolabs; P0753S) for 1 h at 30°C. Phosphatase reactions were stopped by adding an equal volume of 2 × Laemmli buffer and incubation at 95°C for 3 min.

Quick TAP purification

cdc13-1 EXO1-tap::URA3 (DLY2998) strain (61) was grown at 23°C in YPD medium until OD₆₀₀ reached 0.8. A portion of 3 l was incubated further for 3 h at 23°C and 3 l was incubated in parallel at 36°C for 3 h to induce telomere uncapping. A *cdc13-1 EXO1-tap::URA3 pep4Δ* (DLY3280) strain was incubated for 4 h at 36°C. Cells were harvested and washed twice with chilled water and once with lysis buffer LB (Hepes 20 mM, NaCl 0.15 M, glycerol 10%, Tween 0.1%). Pellets were resuspended in 20 ml of LB containing 1 mM phenylmethylsulphonyl fluoride, one tablet antiprotease complete (Roche Applied Science), NaF 1 mM, Naβ glycerophosphate 0.8 mM, 400 μl of cocktail antiphosphatase IV (Merck; 524628) and 330 μl of cocktail antiphosphatase II (Sigma; P5726) and dripped into liquid nitrogen. Cells were disrupted by grinding in a mechanical pestle and mortar as described previously (Caspari *et al*, 2000). To purify TAP-tagged proteins, powdered cell lysates were thawed at 4°C and a volume of 10 ml of lysis buffer was added to the cell extracts. The lysates were clarified by spinning at 13 000 r.p.m. for 10 min. Proteins were immunoprecipitated by incubation at 4°C for 2 h with 450 μl of IgG (rabbit gamma globulin; Invitrogen)-coupled Dynal beads (Dynabeads-M-280 Tosylactivated; Invitrogen; 142-03) pre-equilibrated into lysis buffer. Beads were recovered and washed six times with 3 ml of lysis buffer. Beads were then resuspended in 30 μl of Laemmli buffer and boiled for 10 min at 75°C. The supernatant was loaded in a 7.5% SDS-PAGE (Tris-glycine, 7.5%; Bio-Rad; 161-1172). Gels were stained for 2 h with Brilliant Blue G-Colloidal (Sigma; B-2025) and bands were excised and subjected to MALDI-TOF mass spectrometry.

Proteomic analysis

Tryptic digests were separated on a 150 × 0.075 μm Vydac C18 column (Grace Analytical) equilibrated in 2% acetonitrile/0.1% formic acid and the column was developed with a linear 2–40% acetonitrile gradient in 40 min at 300 nl/min. The masses of potential tryptic phosphopeptides detected by precursor ion scanning were calculated to 10 p.p.m. mass accuracy and entered into an inclusion list. Precursors were analysed in the orbitrap set to a resolution of 60 000 and tandem MS/MS was performed in the LTQ with multistage activation (MSA) of the precursors and precursor –98/z, as described previously (Schroeder *et al*, 2004). The composite MSA spectra were searched against a local database using Mascot (Matrixscience) run on a local server with the search criteria set to 10 p.p.m. mass accuracy for precursors allowing for one tryptic missed cleavage, carboxyamidomethylation of cysteine, oxidation of methionine and phosphorylation of serine, threonine or tyrosine.

Site-directed mutagenesis

The *EXO1TAP* fusion gene plus 900 bp upstream was amplified by PCR (forward primer 1257: ggaatcagactcgagaattgtcatcttaacaaaggagg and reverse primer 1258: ggatccccgggcttcaggaattcgatatcaagcttcagg) from the strain *cdc13-1 EXO1-tap::HIS3* (DLY2998) and cloned in pCR[®]4-TOPO (Invitrogen; K4575-01). *EcoRV* and *XhoI* restriction sites were inserted into the primers and used to subclone *EXO1-tap* into plasmid pRS413. The resulting plasmid was designated pRS413-Exo1-Tap (pDL1124) and the inserted DNA was sequenced. Using *EcoRV* and *XhoI* restriction sites, the promoter sequence and *EXO1-tap* were subcloned in pRS423 to generate pRS423-Exo1-Tap (pDL1126). *EXO1TAP* gene was also amplified by PCR from the strain *cdc13-1 EXO1-tap::URA3* (DLY2998) using primers carrying *HindIII* restriction sites (forward primer 1259: ccttcaggatctataagcttcataagaataaattga-

tattgc and reverse primer 1260: ctgcaggaattcgatatcaagcttcaggtgactccccgc). A PCR fragment was cloned in pCR[®]4-TOPO for sequencing and subcloned in YEp181PALEH (pYep) using *HindIII* restriction sites (Lowe *et al*, 2004). pYep-Exo1-Tap (pDL1116) allows expression of Exo1Tap under the constitutive *ADHI* promoter. The pRS413-Exo1-Tap (pDL1124) was used as a template to produce mutants by the QuikChange[®] Multi Site-Directed Mutagenesis Kit from Stratagene (200515). The *EXO1* gene was then mutated to generate the desired codon changes corresponding to the following mutations S372A, S372E, S567A, S567E, S587A, S587E, S692A and S692E. Plasmids pRS413-Exo1-4S::A-Tap (pDL1143) and pRS413-Exo1-4S::E-Tap (pDL1145) were obtained and the sequence of mutated *EXO1* was confirmed by sequencing.

Integration of point mutations into the genome

To create strains carrying *exo1-4S::A* and *exo1-4S::E* mutations, *EXO1* gene was first truncated in a strain carrying *cdc13-1* mutation (DLY1108). The *EXO1* truncation cassette was amplified by PCR from plasmid Ycplac33 using primers 1442 (aatccatgattttaccacactctagc caacagagagcccttctctcaagaattagc) and 1439 (gaaaaatatactccgatag aaactgtcagacttaacttctgcccagactcatctcc), and the truncation cassettes were transformed into DLY1108, creating a strain with the entire C terminus of *EXO1* removed, DLY4008 (*cdc13-1 exo1Δ1091–2109::URA3*). The corresponding truncated section of *EXO1* was then replaced by mutated and correct (as a control) versions of *EXO1*. *EXO1*, *exo1-4S::A* and *exo1-4S::E* fragments were amplified by PCR from plasmids pDL1124, pDL1143 and pDL1146, respectively, using primers 1447 (aatccatgattttaccacactctagc caacagagagc) and 1448 (gaaaaatatactccgatagaaactgtcagacttaacttatttatacaaaatgggaa agc). These fragments were then transformed into DLY4008 with a carrier plasmid pRS425 (2 μ, LEU). Leu⁺ transformants were replicated onto 5FOA plates to select for correct replacement transformants. These positive transformants were then confirmed by spot test and DNA sequencing.

Spot tests

Single colonies were inoculated into 2 ml YPD or selective medium (–Leu or –Ura) and incubated at 23°C until saturation. Cells were then diluted to a concentration of 1.5 × 10⁷ cells/ml in the corresponding media. A five-fold dilution series of each of the cultures was prepared in a 96-well plate and 3–5 μl was spotted onto plates using a 48-prong replica-plating device. Plates were incubated for 2–4 days at different temperatures before being photographed.

Supplementary data

Supplementary data are available at *The EMBO Journal* Online (<http://www.embojournal.org>).

Acknowledgements

We gratefully acknowledge members of the Lydall laboratory for support and helpful discussions. We are grateful to Vincent Geli and Yves Corda for the gift of the Rad53KD yeast strain YVG152. We thank Dan Durocher for anti-Rad53 antibodies, Keith Gull for anti-tubulin antibodies, Martine Cuillel and Elisabeth Mintz for YEp181PALEH, Yoshiko Tone for the gift of pUb221 and pUb175. Special thanks to Simon Whitehall for allowing access to his facilities for TAP purification, and John Rouse and Dan Durocher for encouraging collaboration between the Morrice and Lydall laboratories. We especially thank Peter Burgers for critically reading the paper. We are grateful to Cancer Research UK, BBSRC and MRC for support. This study was primarily supported by the Wellcome Trust (075294).

References

- Bermejo R, Doksan Y, Capra T, Katou YM, Tanaka H, Shirahige K, Foiani M (2007) Top1- and Top2-mediated topological transitions at replication forks ensure fork progression and stability and prevent DNA damage checkpoint activation. *Genes Dev* **21**: 1921–1936
- Bertuch AA, Lundblad V (2004) EXO1 contributes to telomere maintenance in both telomerase-proficient and telomerase-deficient *Saccharomyces cerevisiae*. *Genetics* **166**: 1651–1659
- Blackburn EH (2001) Switching and signaling at the telomere. *Cell* **106**: 661–673
- Blackburn EH, Greider CW, Henderson E, Lee MS, Shampay J, Shippen-Lentz D (1989) Recognition and elongation of telomeres by telomerase. *Genome* **31**: 553–560
- Boulton SJ, Jackson SP (1996) Identification of a *Saccharomyces cerevisiae* Ku80 homologue: roles in DNA double strand break rejoining and in telomeric maintenance. *Nucleic Acids Res* **24**: 4639–4648
- Campisi J, Kim SH, Lim CS, Rubio M (2001) Cellular senescence, cancer and aging: the telomere connection. *Exp Gerontol* **36**: 1619–1637

- Caspari T, Dahlen M, Kanter-Smoler G, Lindsay HD, Hofmann K, Papadimitriou K, Sunnerhagen P, Carr AM (2000) Characterization of *Schizosaccharomyces pombe* Hus1: a PCNA-related protein that associates with Rad1 and Rad9. *Mol Cell Biol* **20**: 1254–1262
- Chen SH, Smolka MB, Zhou H (2007) Mechanism of Dun1 activation by Rad53 phosphorylation in *Saccharomyces cerevisiae*. *J Biol Chem* **282**: 986–995
- Cosme-Blanco W, Shen MF, Lazar AJ, Pathak S, Lozano G, Multani AS, Chang S (2007) Telomere dysfunction suppresses spontaneous tumorigenesis *in vivo* by initiating p53-dependent cellular senescence. *EMBO Rep* **8**: 497–503
- Cotta-Ramusino C, Fachinetti D, Lucca C, Doksan Y, Lopes M, Sogo J, Foiani M (2005) Exo1 processes stalled replication forks and counteracts fork reversal in checkpoint-defective cells. *Mol Cell* **17**: 153–159
- de Lange T (2005) Shelterin: the protein complex that shapes and safeguards human telomeres. *Genes Dev* **19**: 2100–2110
- Djojicubroto MW, Choi YS, Lee HW, Rudolph KL (2003) Telomeres and telomerase in aging, regeneration and cancer. *Mol Cell* **15**: 164–175
- Dubrana K, van Attikum H, Hediger F, Gasser SM (2007) The processing of double-strand breaks and binding of single-strand-binding proteins RPA and Rad51 modulate the formation of ATR-kinase foci in yeast. *J Cell Sci* **120**: 4209–4220
- El-Shemerly M, Hess D, Pyakurel AK, Moselhy S, Ferrari S (2008) ATR-dependent pathways control hEXO1 stability in response to stalled forks. *Nucleic Acids Res* **36**: 511–519
- El-Shemerly M, Janscak P, Hess D, Jiricny J, Ferrari S (2005) Degradation of human exonuclease 1b upon DNA synthesis inhibition. *Cancer Res* **65**: 3604–3609
- Elledge SJ (1996) Cell cycle checkpoints: preventing an identity crisis. *Science* **274**: 1664–1672
- Enomoto S, Glowczewski L, Lew-Smith J, Berman JG (2004) Telomere cap components influence the rate of senescence in telomerase-deficient yeast cells. *Mol Cell Biol* **24**: 837–845
- Fiorentini P, Huang KN, Tishkoff DX, Kolodner RD, Symington LS (1997) Exonuclease I of *Saccharomyces cerevisiae* functions in mitotic recombination *in vivo* and *in vitro*. *Mol Cell Biol* **17**: 2764–2773
- Fisher TS, Zakian VA (2005) Ku: a multifunctional protein involved in telomere maintenance. *DNA Repair (Amst)* **4**: 1215–1226
- Foiani M, Marini F, Gamba D, Lucchini G, Plevani P (1994) The B subunit of the DNA polymerase alpha-primase complex in *Saccharomyces cerevisiae* executes an essential function at the initial stage of DNA replication. *Mol Cell Biol* **14**: 923–933
- Garvik B, Carson M, Hartwell L (1995) Single-stranded DNA arising at telomeres in *cdc13* mutants may constitute a specific signal for the RAD9 checkpoint. *Mol Cell Biol* **15**: 6128–6138
- Hockemeyer D, Sfeir AJ, Shay JW, Wright WE, de Lange T (2005) POT1 protects telomeres from a transient DNA damage response and determines how human chromosomes end. *EMBO J* **24**: 2667–2678
- Hsu HL, Gilley D, Blackburn EH, Chen DJ (1999) Ku is associated with the telomere in mammals. *Proc Natl Acad Sci USA* **96**: 12454–12458
- Ijima AS, Greider CW (2003) Short telomeres induce a DNA damage response in *Saccharomyces cerevisiae*. *Mol Biol Cell* **14**: 987–1001
- Ivanov EL, Sugawara N, White CI, Fabre F, Haber JE (1994) Mutations in XRS2 and RAD50 delay but do not prevent mating-type switching in *Saccharomyces cerevisiae*. *Mol Cell Biol* **14**: 3414–3425
- Jeggo PA (1998) Identification of genes involved in repair of DNA double-strand breaks in mammalian cells. *Radiat Res* **150**: S80–S91
- Jia X, Weinert T, Lydall D (2004) Mec1 and Rad53 inhibit formation of single-stranded DNA at telomeres of *Saccharomyces cerevisiae* *cdc13-1* mutants. *Genetics* **166**: 753–764
- Johnston LH, Nasmyth KA (1978) *Saccharomyces cerevisiae* cell cycle mutant *cdc9* is defective in DNA ligase. *Nature* **274**: 891–893
- Kolodner RD, Putnam CD, Myung K (2002) Maintenance of genome stability in *Saccharomyces cerevisiae*. *Science* **297**: 552–557
- Lee SE, Moore JK, Holmes A, Umez K, Kolodner RD, Haber JE (1998) *Saccharomyces* Ku70, mre11/rad50 and RPA proteins regulate adaptation to G2/M arrest after DNA damage. *Cell* **94**: 399–409
- Lee SJ, Schwartz MF, Duong JK, Stern DF (2003) Rad53 phosphorylation site clusters are important for Rad53 regulation and signaling. *Mol Cell Biol* **23**: 6300–6314
- Lewis LK, Karthikeyan G, Westmoreland JW, Resnick MA (2002) Differential suppression of DNA repair deficiencies of yeast *rad50*, *mre11* and *xrs2* mutants by EXO1 and TLC1 (the RNA component of telomerase). *Genetics* **160**: 49–62
- Llorente B, Symington LS (2004) The Mre11 nuclease is not required for 5' to 3' resection at multiple HO-induced double-strand breaks. *Mol Cell Biol* **24**: 9682–9694
- Longhese MP, Foiani M, Muzi-Falconi M, Lucchini G, Plevani P (1998) DNA damage checkpoint in budding yeast. *EMBO J* **17**: 5525–5528
- Longtine MS, McKenzie III A, Demarini DJ, Shah NG, Wach A, Brachat A, Philippsen P, Pringle JR (1998) Additional modules for versatile and economical PCR-based gene deletion and modification in *Saccharomyces cerevisiae*. *Yeast* **14**: 953–961
- Lowe J, Vieyra A, Catty P, Guillain F, Mintz E, Cuillel M (2004) A mutational study in the transmembrane domain of Ccc2p, the yeast Cu(I)-ATPase, shows different roles for each Cys-Pro-Cys cysteine. *J Biol Chem* **279**: 25986–25994
- Lydall D, Weinert T (1995) Yeast checkpoint genes in DNA damage processing: implications for repair and arrest. *Science* **270**: 1488–1491
- Majka J, Niedziela-Majka A, Burgers PM (2006) The checkpoint clamp activates Mec1 kinase during initiation of the DNA damage checkpoint. *Mol Cell* **24**: 891–901
- Mann M, Jensen ON (2003) Proteomic analysis of post-translational modifications. *Nat Biotechnol* **21**: 255–261
- Maringele L, Lydall D (2002) EXO1-dependent single-stranded DNA at telomeres activates subsets of DNA damage and spindle checkpoint pathways in budding yeast *yku70Delta* mutants. *Genes Dev* **16**: 1919–1933
- Maringele L, Lydall D (2004) EXO1 plays a role in generating type I and type II survivors in budding yeast. *Genetics* **166**: 1641–1649
- Nugent CI, Hughes TR, Lue NF, Lundblad V (1996) Cdc13p: a single-strand telomeric DNA-binding protein with a dual role in yeast telomere maintenance. *Science* **274**: 249–252
- Nyberg KA, Michelson RJ, Putnam CW, Weinert TA (2002) Toward maintaining the genome: DNA damage and replication checkpoints. *Annu Rev Genet* **36**: 617–656
- Pang TL, Wang CY, Hsu CL, Chen MY, Lin JJ (2003) Exposure of single-stranded telomeric DNA causes G2/M cell cycle arrest in *Saccharomyces cerevisiae*. *J Biol Chem* **278**: 9318–9321
- Pommier Y, Redon C, Rao VA, Seiler JA, Sordet O, Takemura H, Antony S, Meng L, Liao Z, Kohlhaagen G, Zhang H, Kohn KW (2003) Repair of and checkpoint response to topoisomerase I-mediated DNA damage. *Mutat Res* **532**: 173–203
- Puig O, Caspary F, Rigaut G, Rutz B, Bouveret E, Bragado-Nilsson E, Wilm M, Seraphin B (2001) The tandem affinity purification (TAP) method: a general procedure of protein complex purification. *Methods* **24**: 218–229
- Rigaut G, Shevchenko A, Rutz B, Wilm M, Mann M, Seraphin B (1999) A generic protein purification method for protein complex characterization and proteome exploration. *Nat Biotechnol* **17**: 1030–1032
- Rouse J, Jackson SP (2002) Interfaces between the detection, signaling, and repair of DNA damage. *Science* **297**: 547–551
- Sanchez Y, Desany BA, Jones WJ, Liu Q, Wang B, Elledge SJ (1996) Regulation of RAD53 by the ATM-like kinases MEC1 and TEL1 in yeast cell cycle checkpoint pathways. *Science* **271**: 357–360
- Schaetzlein S, Kodandaramireddy NR, Ju Z, Lechel A, Stepczynska A, Lilli DR, Clark AB, Rudolph C, Wei K, Schlegelberger B, Schirmacher P, Kunkel TA, Greenberg RA, Edelmann W, Rudolph KL (2007) Exonuclease-1 deletion impairs DNA damage signaling and prolongs lifespan of telomere-dysfunctional mice. *Cell* **130**: 863–877
- Schmutte C, Sadoff MM, Shim KS, Acharya S, Fishel R (2001) The interaction of DNA mismatch repair proteins with human exonuclease I. *J Biol Chem* **276**: 33011–33018
- Schroeder MJ, Shabanowitz J, Schwartz JC, Hunt DF, Coon JJ (2004) A neutral loss activation method for improved phosphopeptide sequence analysis by quadrupole ion trap mass spectrometry. *Anal Chem* **76**: 3590–3598
- Smolka MB, Albuquerque CP, Chen SH, Zhou H (2007) Proteome-wide identification of *in vivo* targets of DNA damage checkpoint kinases. *Proc Natl Acad Sci USA* **104**: 10364–10369

- Sun Z, Fay DS, Marini F, Foiani M, Stern DF (1996) Spk1/Rad53 is regulated by Mec1-dependent protein phosphorylation in DNA replication and damage checkpoint pathways. *Genes Dev* **10**: 395–406
- Sweeney FD, Yang F, Chi A, Shabanowitz J, Hunt DF, Durocher D (2005) *Saccharomyces cerevisiae* Rad9 acts as a Mec1 adaptor to allow Rad53 activation. *Curr Biol* **15**: 1364–1375
- Tishkoff DX, Boerger AL, Bertrand P, Filosi N, Gaida GM, Kane MF, Kolodner RD (1997) Identification and characterization of *Saccharomyces cerevisiae* EXO1, a gene encoding an exonuclease that interacts with MSH2. *Proc Natl Acad Sci USA* **94**: 7487–7492
- Tran PT, Erdeniz N, Dudley S, Liskay RM (2002) Characterization of nuclease-dependent functions of Exo1p in *Saccharomyces cerevisiae*. *DNA Repair (Amst)* **1**: 895–912
- Tran PT, Erdeniz N, Symington LS, Liskay RM (2004) EXO1-A multi-tasking eukaryotic nuclease. *DNA Repair (Amst)* **3**: 1549–1559
- Tran PT, Simon JA, Liskay RM (2001) Interactions of Exo1p with components of MutLalpha in *Saccharomyces cerevisiae*. *Proc Natl Acad Sci USA* **98**: 9760–9765
- Tsolou A, Lydall D (2007) Mrc1 protects uncapped budding yeast telomeres from exonuclease EXO1. *DNA Repair (Amst)* **6**: 1607–1617
- Tsubouchi H, Ogawa H (2000) Exo1 roles for repair of DNA double-strand breaks and meiotic crossing over in *Saccharomyces cerevisiae*. *Mol Biol Cell* **11**: 2221–2233
- Vega LR, Phillips JA, Thornton BR, Benanti JA, Onigbanjo MT, Toczyski DP, Zakian VA (2007) Sensitivity of yeast strains with long G-tails to levels of telomere-bound telomerase. *PLoS Genet* **3**: e105
- Wang HC, Chou WC, Shieh SY, Shen CY (2006) Ataxia telangiectasia mutated and checkpoint kinase 2 regulate BRCA1 to promote the fidelity of DNA end-joining. *Cancer Res* **66**: 1391–1400
- Wang X, Haber JE (2004) Role of *Saccharomyces* single-stranded DNA-binding protein RPA in the strand invasion step of double-strand break repair. *PLoS Biol* **2**: E21
- Williamson BL, Marchese J, Morrice NA (2006) Automated identification and quantification of protein phosphorylation sites by LC/MS on a hybrid triple quadrupole linear ion trap mass spectrometer. *Mol Cell Proteomics* **5**: 337–346
- Zhao X, Muller EG, Rothstein R (1998) A suppressor of two essential checkpoint genes identifies a novel protein that negatively affects dNTP pools. *Mol Cell* **2**: 329–340
- Zhuang J, Zhang J, Willers H, Wang H, Chung JH, van Gent DC, Hallahan DE, Powell SN, Xia F (2006) Checkpoint kinase 2-mediated phosphorylation of BRCA1 regulates the fidelity of nonhomologous end-joining. *Cancer Res* **66**: 1401–1408
- Zou L, Elledge SJ (2003) Sensing DNA damage through ATRIP recognition of RPA–ssDNA complexes. *Science* **300**: 1542–1548
- Zubko MK, Guillard S, Lydall D (2004) Exo1 and Rad24 differentially regulate generation of ssDNA at telomeres of *Saccharomyces cerevisiae* cdc13-1 mutants. *Genetics* **168**: 103–115



The EMBO Journal is published by Nature Publishing Group on behalf of European Molecular Biology Organization. This article is licensed under a Creative Commons Attribution-NonCommercial-Share Alike 3.0 Licence. [<http://creativecommons.org/licenses/by-nc-sa/3.0/>]